ACS APPLIED MATERIALS & INTERFACES

Research Article

www.acsami.org

Colorimetric Disposable Paper Coated with ZnO@ZnS Core–Shell Nanoparticles for Detection of Copper Ions in Aqueous Solutions

Azar Sadollahkhani,*[,†,§] Amir Hatamie,[†,‡] Omer Nur,[†] Magnus Willander,[†] Behrooz Zargar,[‡] and Iraj Kazeminezhad[§]

[†]Department of Science and Technology, Campus Norrköping, Linköping University, SE-60174 Norrköping, Sweden

[‡]Department of Chemistry, Faculty of Sciences, and [§]Nanotechnology Lab, Department of Physics, Shahid Chamran University, Ahvaz, Iran

ABSTRACT: In this study, we have proposed a new nanoparticle-containing test paper sensor that could be used as an inexpensive, easy-to-use, portable, and highly selective sensor to detect Cu^{2+} ions in aqueous solutions. This disposable paper sensor is based on ZnO@ZnS core–shell nanoparticles. The core–shell nanoparticles were synthesized using a chemical method and then they were used for coating the paper. The synthesis of the ZnO@ZnS core–shell nanoparticles was performed at a temperature as low as 60 °C, and so far this is the lowest temperature for the synthesis of such core–shell nanoparticles. The sensitivity of the paper sensor was investigated for different Cu^{2+} ion concentrations in aqueous solutions and the results show a direct linear relation between the Cu^{2+} ions concentration and the color intensity of the paper sensor with a visual detection limit as low as 15 μM (~0.96 ppm). Testing the present paper sensor on real river turbulent water shows a maximum 5% relative error for determining the Cu^{2+} ions concentration, which confirms that the presented paper sensor can successfully be used efficiently for detection in complex solutions with high selectivity. Photographs of the paper sensor taken using a regular digital camera were transferred to a computer and analyzed by ImageJ Photoshop software. This finding demonstrates the potential of the present disposable paper sensor for the development of a portable, accurate, and selective heavy metal detection technology.

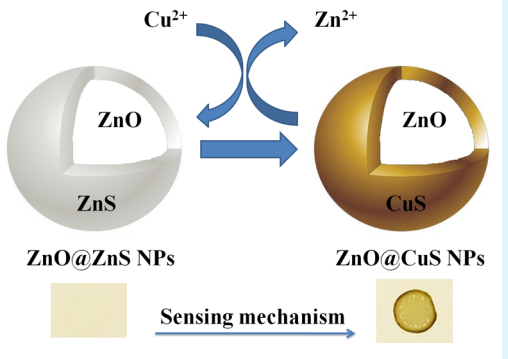

KEYWORDS: *colorimetric detection, copper ion, core–shell nanoparticles, ImageJ software*

INTRODUCTION

In recent years, the sensing and recognition of cations and anions has emerged as a key research field within chemistry because of the important role of cations and anions in a wide range of industrial, environmental problems, and for biological systems.[1,2] Therefore, the recognition and sensing of the cationic and anionic analysts has attracted considerable attention as a significant goal of research programs.[3−5] Among the different methods for sensing cationic and anionic analysts, colorimetric sensors have attracted more attention, becaues of their simplicity, rapidity, precision, and common availability of the basic equipment in laboratory and field research.[6−11] Furthermore, colorimetric methods are extremely attractive in the field of detection, because the read out is easy. It can be performed using the naked eye, offering advantages of simplicity and rapidity, along with the additional benefits of cost-effectiveness and no requirement of any sophisticated instrumentation.[12,13] Recently, paper-based analytical devices have gained great interest because of their attractive advantages, such as low cost and simplicity. Compared to the conventional analytical methods that require complex instrumentation, paper based analytical devices are usually integrated with simple colorimetric detection systems.[7,8]

Heavy metal ions such as Cu^{2+}, Zn^{2+}, Cd^{2+}, and Hg^{2+} represent a threat to human health and the whole environment and for this reason they have attracted a lot of attention in different research fields.[14] Copper, the third most abundant transition metal ions in the human body, plays an important role in a variety of fundamental biological processes in organisms and acts as an essential trace element. Nevertheless, copper with high concentrations can induce toxic effects in living organisms and cause severe diverse effects in humans. For instance, excess copper in drinking water has been suspected of causing liver cirrhosis in children, and has been linked to serious neuro-degenerative diseases.[15−17] Therefore, excess amount of copper can threaten human health, and hence copper removal from drinking water is an important issue that must be considered. For this purpose, the first step is the detection and the accurate quantification of Cu^{2+} ions in drinking water. Although some studies have been conducted in this area and some methods have been demonstrated for the detection of the Cu^{2+} ions in the water,[18−21] there is still a lack of a portable, disposable, highly sensitive and selective, and easy-to-use sensor based on a colorimetric response that is usable with naked eyes. Such disposable detection method will be useful for the public and

Received: June 23, 2014
Accepted: October 2, 2014
Published: October 2, 2014

especially in remote areas where drinking water is supplied from local wells and small running streams.

Nowadays, nanomaterials have attracted extensive interest in modern chemistry because of their unique superior properties for optical, electronic, magnetic, and catalytic effects. Among the different nanomaterials, zinc oxide nanoparticles (ZnO NPs) have their own importance because of their vast area of applications, such as chemical and biosensing, cosmetics, optical and electrical devices, drug-delivery, solar cells, etc.[22,23] Also, covering ZnO NPs with another material can tune its properties to make it useful in other research area.[24] Nowadays, considerable effort has been devoted to the design and fabrication control of ZnO@ZnS CSNPs. Various ZnO@ZnS core−shell nanostructures have been synthesized, most of them at elevated temperature.[25] Epitaxial growth of ZnS shell on ZnO core is obtained by the high-temperature synthesis. In contrast, low-temperature synthesis with low cost can lead to a uniform nanocrystalline ZnS structure, but so far only a limited number of publications can be found.[26] There is a lack of simple and fast reliable way for the growth of pure ZnO@ZnS CSNPs with full coverage of the shell material. In the work reported by Nam et al.[27] the starting materials and the method are different from the present manuscript, and the grown ZnO@ZnS CSNPs are quite larger in size (more than 200 nm) compared to the core−shell nanoparticles presented in this work. Sharma et al.[28] the reported a preparation method of the ZnO@ZnS CSNPs using the same precursors as ours, whereas their HRTEM results show a nonuniform core/shell NPs. Liu et al. successfully obtained a full coverage of ZnS shell at low temperature, but with a more time-consuming process than presented herein.[29] Recently, Wenjiang et. al reported the synthesis of ZnS@ZnO CSNPs using the hydrothermal chemical growth using a temperature as high as 160 °C.[30] For utilizing ZnO@ZnS CSNPs on any type of soft substrate, it would be of interest to reduce the synthesis temperature much below 160 °C.

In this research paper, we have fabricated an easy-to-use and highly selective and sensitive test paper based on ZnO@ZnS core−shell nanoparticles (CSNPs) synthesized using the chemical approach at a temperature as low as 60 °C. This low-temperature synthesis is, as far as we know, the lowest temperature reported for the synthesis of such CSNPs. The developed paper sensor can detect Cu^{2+} in aqueous solutions. The demonstrated paper sensor indicates the potential application for detecting Cu^{2+} in the aqueous environmental samples, e.g., fresh drinking water, without any spectroscopic instrumentation. The color intensity of the paper sensor can be monitored by the naked eyes. The pictures of the test papers were taken with a regular digital camera and transferred to the computer and analyzed by ImageJ Photoshop software. An observed direct linear relation between the color intensity and the Cu^{2+} concentration shows that increase in the Cu^{2+} concentration in the solution leads to enhancement of the color intensity. Eventually, to indicate the superiority of using ZnO@ZnS CSNPs, we investigated the utility of using ZnO nanoparticles (NPs) and compared it to the CSNPs. It was found that pure ZnS NPs do not disperse uniformly in aqueous water solutions as compared to the ZnO@ZnS CSNPs and subsequently cannot create a uniform spot on the paper sensor.

2. EXPERIMENTAL SECTION

2.1. Chemicals and Materials. Zinc acetate dehydrates ($ZnAC_2.2H_2O$) and sodium hydroxide (NaOH) were used as the starting materials for preparing the ZnO NPs and sodium sulfide (Na_2S), zinc chloride ($ZnCl_2$) and isopropanol were used as precursors for covering the ZnO NPs with ZnS. Copper nitrate trihydrate was used to prepared different solution with various Cu^{2+} concentrations to study the colorimetric responses of the paper sensor. All chemicals were of analytical grade and were purchased from Sigma-Aldrich. Filter paper with 0.22 μm pore size was purchased from Millipore for making the paper sensors.

2.2. Instruments. The structural characteristics of the ZnO@ZnS CSNP and the paper sensor were investigated by X-ray powder diffraction (XRD) using a Phillips PW 1729 powder diffractometer equipped with CuKα radiation (λ = 1.5418 Å) operating at a generator voltage of 40 kV and a current of 40 mA. The high-resolution transmission electron microscopy (HRTEM) characterization was carried out using a FEI Tecnai G2 TF20 UT instrument with a field-emission gun operated at 200 kV. The instrument has a point resolution of 0.19 nm and is equipped with an EDX system. The TEM specimen was prepared by dispersing the nanostructure powder on a copper grid with a thin amorphous carbon film. Photographic results were recorded using a 13 Megapixel camera of the Galaxy Note III and were analyzed with a ImageJ software.

2.3. Synthesize of ZnO NPs and ZnO@ZnS CSNPs. To grow ZnO NPs, we dissolved zinc acetate dehydrate and sodium hydroxide in deionized water to form two transparent solutions with 0.5 and 1 M concentrations, respectively, and then added them dropwise into a beaker at room temperature. After 2 h of stirring, the obtained precipitation was separated by centrifugation. Finally, the precipitation was washed with deionized water and acetone and was dried at 75 °C. Covering the ZnO NPs with the ZnS was performed by adding 0.30 g of the as-grown ZnO NPs to 50 mL of isopropanol and sonication for 10 min. After adjusting the pH at 10, we added a solution of Na_2S to the mixture dropwise. The solution was stirred for 2 h at 60 °C, and then a solution of 0.05 M $ZnCl_2$ was added dropwise into the above mixture and stirred for 1 h. Afterward, the product was washed with deionized water and acetone and dried at 70 °C.

2.4. Preparation of Paper Sensor. To prepare the sensor for the detection of Cu^{2+} ions, a uniform and soft surface that is fully covered with the ZnO@ZnS CSNPs is needed. Using a relatively large amount of ZnO@ZnS CSNPs can lead to the formation of a large and nonuniform surface, which usually results in nonconcentrated color intensity from the samples under investigation and causes some difficulties for analyzing the data. To make the paper sensor, we prepared a 0.5% (W/V) solution of the as-grown ZnO@ZnS CSNPs. The uniform solution was obtained after 5 min ultrasonication and 30 min stirring alternatively. Then 10 μL of the mentioned solution was dropped on a piece of paper and was kept at room temperature for 30 min to dry. Different solutions with various Cu^{2+} concentrations (15, 75, 150, 300, 450, 750, and 1500 μM) were prepared to investigate the colorimetric responses of the paper sensor. All the experimental solutions were prepared using deionized water (18 MΩ resistivity) and for testing the paper sensor in a complex solution, a Cu^{2+} solution with three different concentrations was prepared using turbulent real water from Motala Stream River in Norrkoping city, Sweden. The samples were photographed by a 13 Megapixel camera of the Galaxy Note III with auto mode. In order to measure the color intensity of the images, the pictures were transferred to a computer and analyzed by ImageJ Photoshop software. The analysis was carried out based on the color intensity of each picture. This program has the ability of measuring the color intensity at a specific region with desired size. So the same region of each spot (center of the spot) with the same size (36 × 36 pixels) was analyzed to determine the color intensity. The choice of the region from the center was adopted to avoid edges of the circle which have a different concentration compared to the center. The output results obtained from the ImageJ software are collected in two different forms. One shows the color intensity qualitatively, and also the software give us another outputs such as color intensity value, which is a number to show the color intensity quantitatively. It is important here to mention that the value of the intensity collected by the Camera depends on the lighting intensity in the medium of measurement. Nevertheless, the software can be calibrated to consider the medium condition(s) to provide real adjusted values.

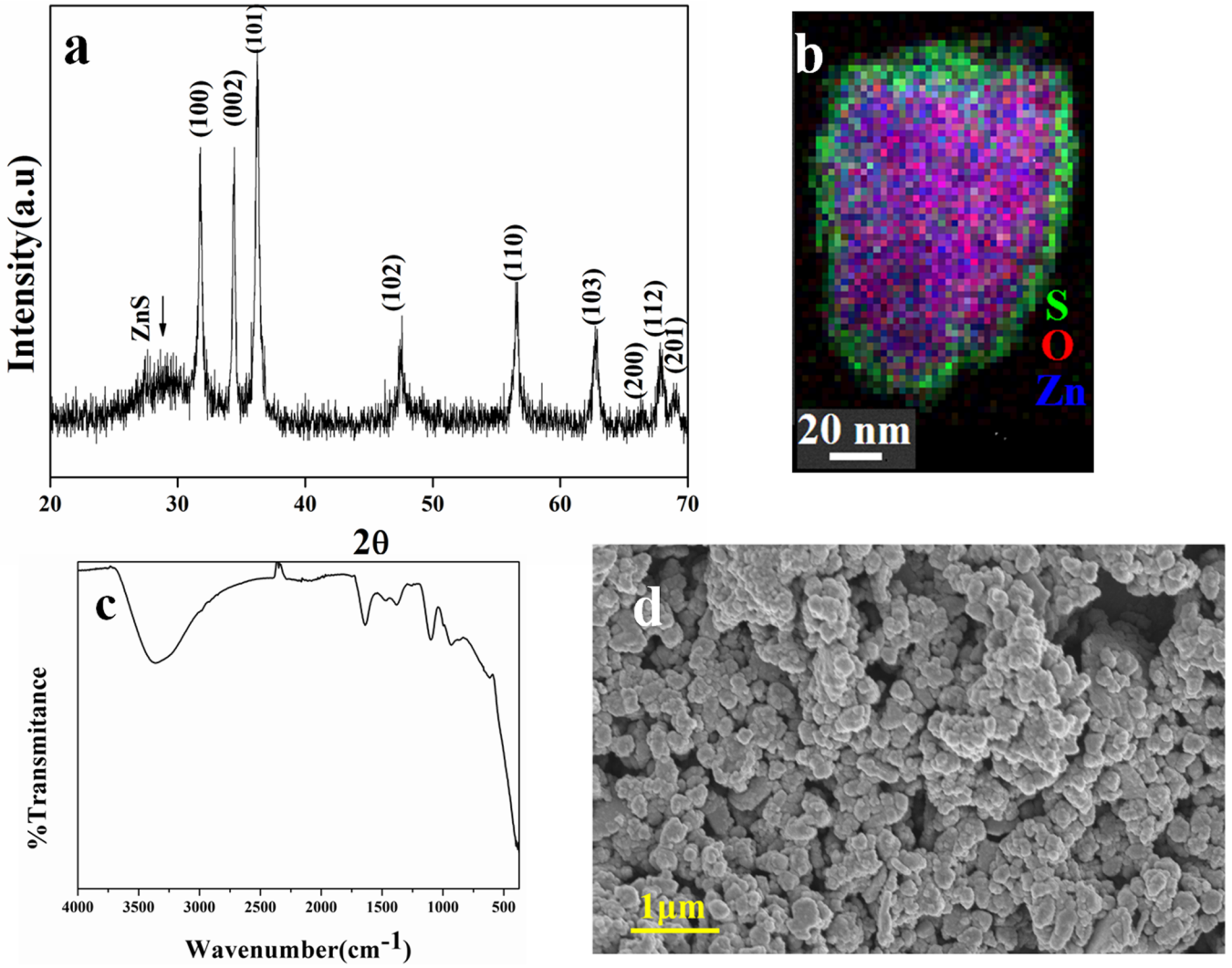

Figure 1. (a) XRD spectrum, (b) TEM image, (c) ATR-FTIR spectrum, and (d) SEM image of ZnO@ZnS CSNPs.

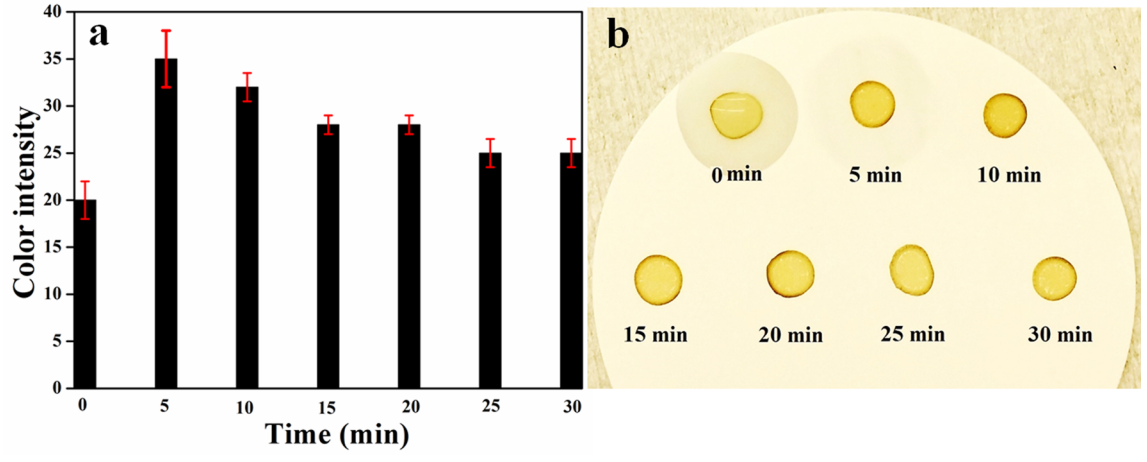

Figure 2. (a) Column plot of the color intensity versus time, and (b) changes of the filter paper every 5 min.

3. RESULTS AND DISCUSSION

3.1. Characterization of the ZnO@ZnS CSNPs. The XRD pattern of the ZnO@ZnS CSNPs is shown in Figure 1a. As it is clear the peaks of the ZnO NPs can be indexed to the known hexagonal wurtzite structure with lattice constants of $a = b =$ 3.250 Å and c = 5.207 Å (JCPDF: 79−2205). Furthermore, a wide peak at 29° belongs to the ZnS (JCPDF: 50566) indicating the coverage the ZnO NPs with ZnS. EDX mapping when using the HRTEM was performed to confirm that the ZnO core structure is fully covered by a ZnS shell and is shown in Figure 1b. The distribution of sulfur, oxygen, and zinc confirms that the

dx.doi.org/10.1021/am505480y | ACS Appl. Mater. Interfaces 2014, 6, 17694−17701

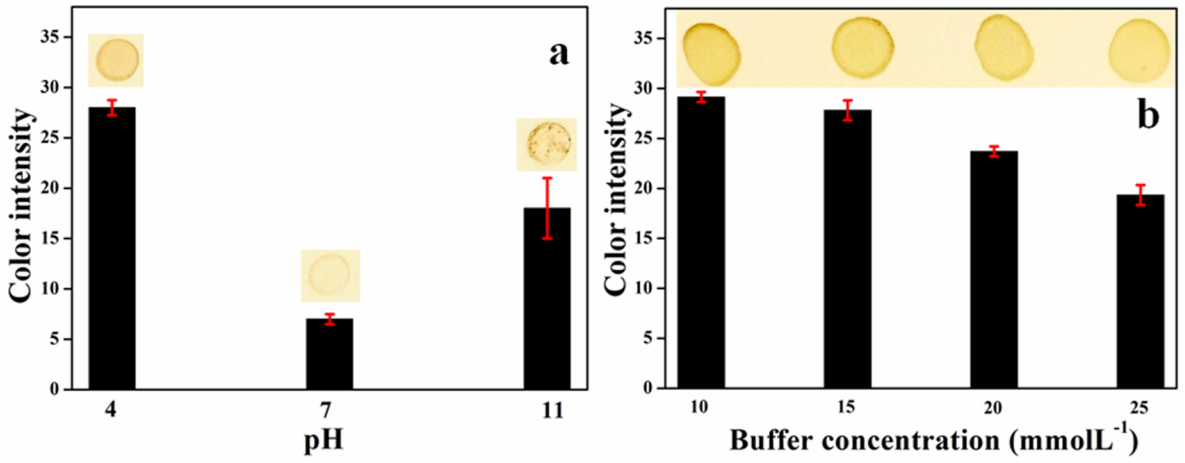

Figure 3. (a) Column plot of color intensity at different pH, and (b) the column plot of color intensity for different buffer concentrations.

ZnO as a core is completely surrounded by the ZnS as a shell. Further information about the surface of ZnO@ZnS CSNPs was found using ATR-FTIR. As it can be seen from Figure 1c, the peak at around 1100 cm^{-1} is the ZnS vibration peak and exhibits that the ZnO nanoparticles is capped with ZnS. Moreover, the peak which is observed from 400 to 500 cm^{-1} is due to Zn−O vibrations of ZnO NPs. SEM image was prepared to investigate the morphology and the uniformity of the ZnO@ZnS CSNPs and is shown in Figure 1d.

3.2. Colorimetric Measurements. Because the aim of this work was to demonstrate a portable and easy-to-use paper sensor for the detection of Cu^{2+} ions in drinking water, the steady state reaction time between Cu^{2+} and the paper sensor must be determined. Moreover, as the pH is an important parameter in redox reactions it is important to determine the optimum pH for the operation of the paper sensor, and the buffer concentration of the Cu^{2+} solution. Then before exploring the sensing activity of the paper sensor, the steady-state time, effect of pH, and the effect of buffer concentration were investigated.

3.2.1. Color Development Time. To investigate the effect of time on the colorimetric response of the paper sensor, we prepared a 1 mM solution of the Cu^{2+} and dropped 20 μL of this solution on the paper sensor. Then the paper sensor was photographed over 30 min with images recorded every 5 min. Figure 2a indicates the column plot of the color intensity versus time and Figure 2b shows the real image of the paper sensor for each time. According to this Figure, after 20 min the changes in color intensity reaches a steady value and we can consider it as a steady-state reaction time and in the subsequence experiments all the pictures are taken after 20 min.

3.2.2. Effect of the pH on the Operation of the Paper Sensor. To specify the optimum pH for the performance of the sensor in the Cu^{2+} solution, i.e., the optimum colorimetric response of the paper sensor, we prepared a solution with 1 mM Cu^{2+} concentration with three different pH values of 4, 7, and 11. Then, a 10 μL of each solution was drop-casted on the paper sensor and dried at room temperature. After 20 min, the samples were photographed and the results were analyzed by the ImageJ Photoshop software to determine the color intensity of the paper sensor for each of the three different pH values. Figure 3a shows the column plot of the color intensity versus pH of the Cu^{2+} solution with the picture of each sample as an inset. It was observed that, at pH 11, the Cu^{2+} ions started to sediment (to form $Cu(OH)_2$) and do not participate in the reaction, so the exact amount of the Cu^{2+} ions could not be detected at this pH value. It is well-known that the pH value of most environmental samples is around 7, but according to our results shown in Figure 3a the best efficiency of the present paper sensor (strongest color intensity) was obtained at pH 4 which shows that the reaction between the Cu^{2+} ions and the paper sensor is more severe at this pH; therefore, a pH value of 4 was selected as an optimum operating pH for further experiments.

3.2.3. Effect of Buffer Concentration. Different buffer concentrations were obtained by preparing 1 mM Cu^{2+} solution at pH 4 with different buffer concentrations (10, 15, 20, and 25 mM). Figure 3b indicates the column plot of color intensity for different buffer concentrations with the image of each sample as an inset. Image analysis shows that the detected Cu^{2+} in the solution with 10 mM buffer concentration indicates the highest intensity compared to the other concentrations and can be considered as a preferable buffer concentration.

3.3. Detection of Cu^{2+} on the Paper Sensor. All the above results show that for getting the best response from the paper sensor the pH and buffer concentration of the Cu^{2+} solution must be adjusted at 4 and 10 mM, respectively, and the samples should be photographed after 20 min.

To determine the response of the paper sensor for detecting the Cu^{2+} in the aqueous solutions with different concentrations, we prepared six different solutions with various concentration of the Cu^{2+} (15, 75, 150, 300, 450, 750, and 1500 μM). As was mentioned above, the pH and the buffer concentration of each solution were adjusted at 4 and 10 mM, respectively. Twenty microliters of each solution was drop-casted on the piece of the paper sensor and after 20 min a photograph was taken using the digital camera. Figure 4a shows the color intensity versus the Cu^{2+} ions concentration obtained by the ImageJ with a digital photograph shown as an inset, whereas Figure 4b indicates the value of the color intensity versus the Cu^{2+} ions concentration. The inset of Figure 4b shows a digital photograph of the paper sensor. Figure 4c shows the calibration curve of the color intensity at different concentrations of the Cu^{2+} ions. According to Figure 4c, the as-prepared paper sensor response to variations of the Cu^{2+} ions concentration is observed to be linear. As shown, when decreasing the concentration of the Cu^{2+} ions in the solution, a decrease in the color intensity was observed, as expected. The linearity of the calibration curve confirms the ability of this paper sensor to measure the concentration of the Cu^{2+} ions in different solutions. Also, the relative standard

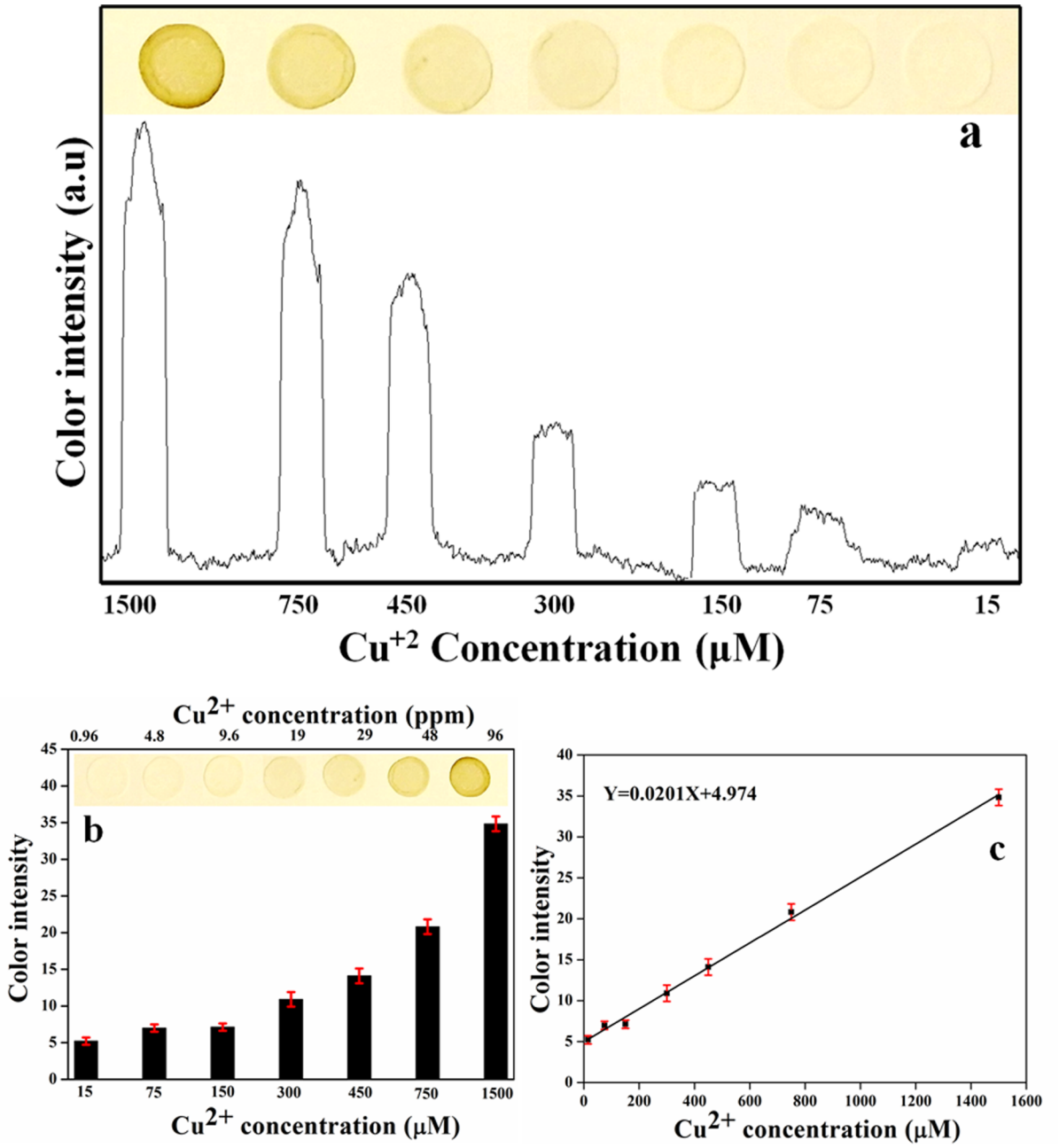

Figure 4. (a) Color intensity versus the Cu^{2+} ions concentration obtained by the ImageJ with a digital photograph as an inset, (b) the value of the color intensity versus the Cu^{2+} ions concentration, and (c) the calibration curve of the color intensity at different concentrations of the Cu^{2+} ions.

deviation was calculated to be 7.1% for the determination of 1000 μM Cu^{2+} and this shows that the sensor has an acceptable precision.

The detection limit of this sensor was found to be about 15 μM, which is lower than the critical standard level of Cu^{2+} allowed in drinking water (WHO standard, 30 μM; EPA and China standard, 20 μM).[19,31,32] Table 1 displays a comparison between the results of the present method and some other reported methods. As can be seen, by applying a simple and fast technique to analyze the data as in this study, we have obtained an acceptable detection limit.

3.4. Paper Sensor Response to Other Cations and Anions. To investigate the practical application, i.e., the selectivity of the paper sensor, it was utilized to sense various cations and anions (Na^+, K^+, Mg^{2+}, Co^{2+}, Ca^{2+}, Ni^{2+}, Al^{3+}, Si^{4+},

Table 1. Comparison of the Results of the Present Sensor with Some Other Published Papers for Cu^{2+} Ion Detection

analytical technique	LDR[a] (μM)	LOD[b] (μM)	ref
proposed method	15−1500	15[c]	this work
colorimetric method: paper sensor	7.8−62.8	not reported	21
colorimetric method: test kit	not reported	0.1	22
spectrophotometry	15.9−126.0	0.4	33
spectrophotometry	not reported	>50.0	34
spectrophotometry	not reported	20[c]	35
spectrophotometry	not reported	14.9[c]	36

[a]LDR: linear dynamic range. [b]LOD: limit of detection.

Fe^{2+}, Fe^{3+}, Cd^{2+}, Cl^{-}, NO_3^{-}, and CO_3^{2-}). A solution with 1.5 mM concentration of each of these cations and anions was prepared at pH 4 with 10 mM of the buffer solution concentration. Then a 20 μL of each solution was dropped on the paper sensor and dried at room temperature. The pictures were taken after 20 min and are shown in Figure 5. As is clear, although the sensor responds to

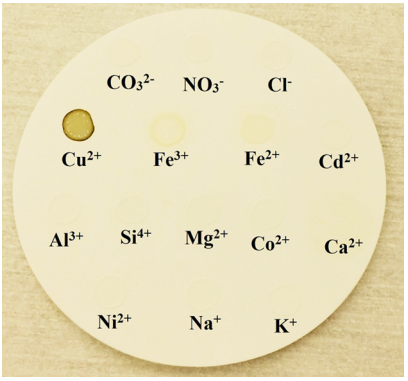

Figure 5. Selectivity of the paper sensor with different cations and anions.

the Fe^{2+}, Fe^{3+} ions, the obvious color change takes place only by adding Cu^{2+} ions. Therefore, this paper sensor could directly detect Cu^{2+} ions in the aqueous solutions without a negative effect from other cations and anions that could be available in the aqueous solution. Hence the present paper sensor possesses a high selectivity for Cu^{2+} ions.

The other disturbing factor that needs to be considered is Humic substances. But as is known, the concentration of these compounds is not too high in aqueous samples, so the amount of water that has been dropped on to the sensor is not enough for these compounds to be enriched onto the present paper sensor.[37,38]

3.5. Analysis of the Real Sample. To investigate the ability of this paper sensor to perform in a solution with different unknown pollutant, we used the water of the Motala stream river (Norrköping, Sweden) as a complex solution. Before preparing the solution, water was tested with the paper sensor and no Cu^{2+} ions were found in the water. Then three solutions with different Cu^{2+} concentrations (1.5 mM, 300 μM, and 75 μM) were prepared and the pH and buffer concentration of them were adjusted at 4 and 10 mM respectively. Twenty microliters of each solution was dropped on the paper sensor and dried at room temperature. The paper sensor was photographed and the pictures were transferred to the computer to calculate the color intensity and measuring the equivalent Cu^{2+} concentration using calibration curve. To compare the color intensity of the real samples to that of the experimental samples that were prepared using deionized water, we show the column plot of color intensity in Figure 6. Table 2 shows the measured Cu^{2+} concentration of each solution using this method and also the relative error of each one. This amount of relative error is acceptable and confirms the practical applicability of this paper sensor to detect Cu^{2+} ions in complicated solutions.

3.6. Comparing the Performance of ZnS NPs and ZnO@ZnS CSNPs as a Cu^{2+} Detection Sensor. ZnS NPs were synthesized using a coprecipitation method.[39] The ability of bare ZnS nanoparticles instead of ZnO@ZnS CSNPs was then studied by preparing the same paper sensor using ZnS NPs. In order to prepare a uniform 0.5 M ZnS solution, the mixture was

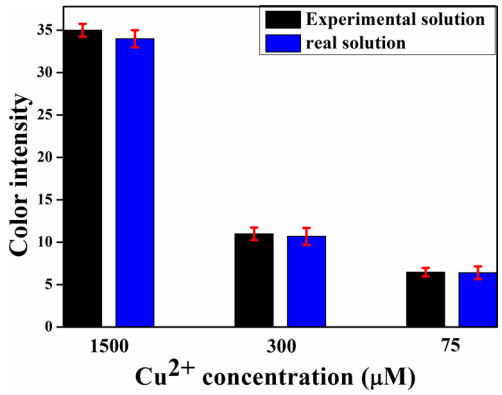

Figure 6. Column plot of the color intensity for the real and the experimental samples.

Table 2. Determination of Cu^{2+} in a River Water Sample by a Standard Addition Method

add Cu^{2+} (μM)	found Cu^{2+} (μM)	recovery (%)	relative error(%)
0	0		
75	71	94.6	5
300	290	96.6	3
1500	1440	96.0	4

stirred for 24 h, after 30 min exposing to the ultrasonic wave. It was observed that the ZnS NPs has limited dispersibility in water compare to the ZnO@ZnS CSNPs which can be dispersed in water after ultrasonication for 5 and 30 min stirring. Ten microliters of the as-prepared ZnS solution was placed on the piece of the paper and dried at room temperature. The sensing activity of the ZnS NPs paper sensor was examined by dropping 20 μL of different solutions with various Cu^{2+} concentrations. Figure 7 shows the colorimetric response of the paper sensor for

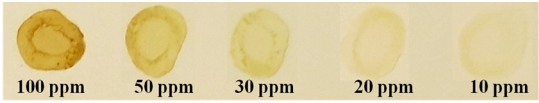

Figure 7. Sensitivity of the paper sensor based on the ZnS NPs for different Cu^{2+} ions concentrations.

different concentration of the Cu^{2+} ions. Because it was not possible to obtain a uniform ZnS solution, the colorimetric response behavior of this paper sensor was not uniform or repeatable. This result show that using a paper sensor coated with ZnO@ZnS CSNPs not only indicates a uniform spot under influence of Cu^{2+} ions, but is easy to prepared because of its uniform dispersibility in water.

4. MECHANISM OF CU^{2+} DETECTION SENSOR

Once the Cu^{2+} was transferred on to the sensor, cation exchange begins at the interface between the ZnO@ZnS CSNPs surface and the Cu^{2+} aqueous solution. The driving force for the cation exchange is provided by the large difference in solubility between the ZnS, and the CuS (solubility product constant (K_{sp}) of ZnS is 2.93×10^{-25} and K_{sp} for CuS is 8×10^{-37}).[40,41] To investigate the mechanism of the present paper sensor for detecting Cu^{2+} ions in aqueous solutions, we measured the XRD spectra of the paper and the paper sensor after and before the addition of the Cu^{2+} ions. According to Figure 8, after the addition of the Cu^{2+} on the

dx.doi.org/10.1021/am505480y | ACS Appl. Mater. Interfaces 2014, 6, 17694−17701

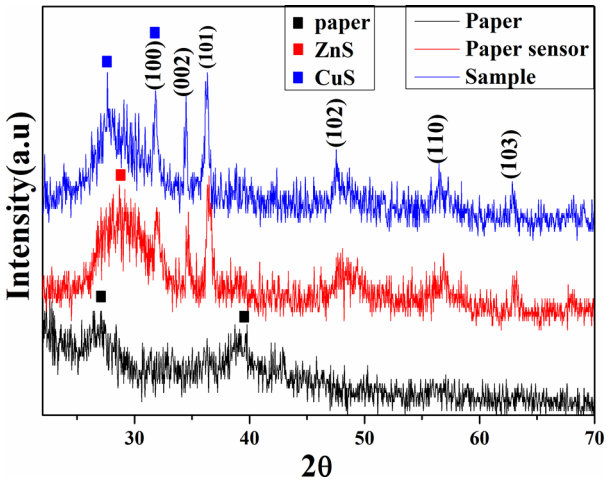

Figure 8. XRD spectra of the paper, paper sensor, and used after adding Cu^{2+} ions.

paper sensor, two additional peaks appeared. A comparison with the standard card (JCPDF: 006−0464) the peak around 27.6° belongs to the CuS crystal plane of (101). Also, a careful perusal of XRD image shows that the intensity of the peak at 32° became higher by adding Cu^{2+} ions. Because the CuS has a peak at this angle that belongs to the (101) crystal plane, we can claim that the reaction between the paper sensor and the Cu^{2+} leads to the formation of CuS and color changing from white to brown confirms this fact.[42] We postulate that the following reaction takes place and the cation in the shell of CSNPs (i.e., the Zn^{2+}) was simply exchanged with the Cu^{2+} ions according to the following reaction:

$$ZnS(s) + Cu^{2+}(aq) \rightarrow CuS(s) + Zn^{2+}(aq)$$

Also, according to the SEM images of the paper (without adding nanoparticles), the paper (after adding nanoparticles) and the used paper (after adding Cu^{2+} ions) shown in Figure 9, adding

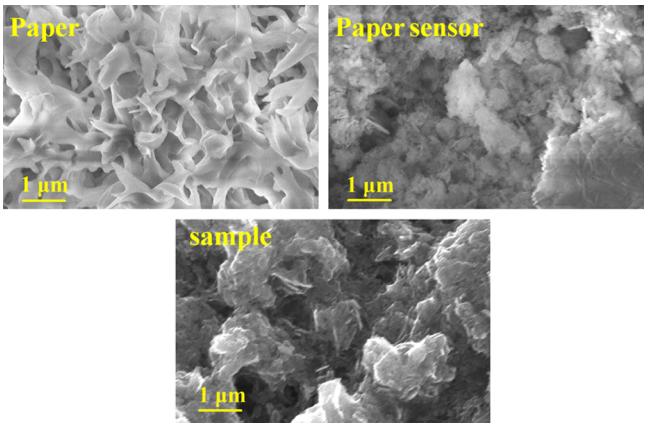

Figure 9. SEM images of the paper, paper sensor, and used paper sensor after adding Cu^{2+} ions.

the Cu^{2+} ions leads to increase the agglomeration. Increasing the agglomeration could be explained by considering the fact that, as the ZnO@ZnS CSNP are accumulated on the paper, by adding the Cu^{2+} to the paper the Cu^{2+} ions will react with a cluster of ZnO@ZnS CSNPs, which can further increase the size and agglomeration.

4. CONCLUSIONS

In this study, a portable, highly sensitive and selective, and easy-to-use paper sensor for detecting Cu^{2+} ions in aqueous solution was prepared using ZnO@ZnS CSNPs. The ZnO@ZnS CSNPs were synthesized using a low temperature chemical method which is fast and easy to use. The grown CSNPs were coated on a paper and were utilized as a disposable paper sensor. The optimum pH and buffer concentration of the Cu^{2+} solution presented here were obtained as 4 and 10 mM, respectively. To investigate the sensing activity, we tested the paper sensor in the presence of different concentration of the Cu^{2+}. The paper sensor was photographed and the results were analyzed using ImageJ software. The results show that increasing the Cu^{2+} concentration leads to linear increase of the color intensity of the paper sensor. Testing the paper sensor in a complex turbulent solution confirmed the practical applicability of the presented disposable paper sensor. The lower limit of detection estimated from the present sensor was 15 μM (~0.96 ppm), which is less than the international allowed level of Cu^{2+} ions in drinking water. The findings and use of CSNPs presented here indicate the potential as the method adopted is low cost and easy and can be scaled up for mass production.

AUTHOR INFORMATION

Corresponding Author

*E-mail: azar.sadollah.khani@liu.se or azarkhanny@gmail.com.

Notes

The authors declare no competing financial interests.

ACKNOWLEDGMENTS

The authors thank Shahid Chamran University and Linkoping Universityfor financial support.

REFERENCES

(1) Cha, R.; Wang, D.; He, Z.; Ni, Y. Development of Cellulose Paper Testing Strips for Quick Measurement of Glucose Using Chromogen Agent. *Carbohydr. Polym.* **2012**, *88*, 1414−1419.

(2) Zargar, B.; Hatamie, A. Localized Surface Plasmon Resonance of Gold Nanoparticles as Colorimetric Probes for Determination of Isoniazid in Pharmacological Formulation. *Spectrochim. Acta, Part A* **2013**, *106*, 185−189.

(3) Liu, J. M.; Wang, X. X.; Jiao, L.; Cui, M. L.; Lin, L. P.; Zhang, L. H.; Jiang, S. L. Ultra-Sensitive Non-Aggregation Colorimetric Sensor for Detection of Iron Based on the Signal Amplification Effect of Fe^{3+} Catalyzing H_2O_2 Oxidize Goldnanorods. *Talanta* **2013**, *116*, 199−204.

(4) Hajizadeh, S.; Farhadi, K.; Forough, M.; Sabzi, R. E. Silver Nanoparticles as a Cyanide Colorimetric sensor in Aqueous Media. *Anal. Methods* **2011**, *3*, 2599−2603.

(5) Liu, X.; Lin, Q.; Wei, T. B.; Zhang, Y. M. A Highly Selective Colorimetric Chemosensor for Detection of Nickel Ions in Aqueous Solution. *New J. Chem.* **2014**, *38*, 1418.

(6) Ke, J.; Li, X.; Shi, Y.; Zhao, Q.; Jiang, X. A Facile and Highly Sensitive Probe for Hg(II) Based on Metal-Induced Aggregation of ZnSe/ZnS Quantum Dots. *Nanoscale* **2012**, *4*, 4996−5001.

(7) Kim, H.; Na, Y. J.; Song, E. J.; Kim, K. B.; Bae, L. M.; Kim, C. A Single Colorimetric Sensor for Multiple Target Ions: the Simultaneous Detection of Fe^{2+} and Cu^{2+} in Aqueous Media. *RSC Adv.* **2014**, *4*, 22463−22469.

(8) Cate, D. M.; Dungchai, W.; Cunningham, J. C.; Volckens, J.; Henry, C. S. Simple, Distance-Based Measurement for Paper Analytical Devices. *Lab Chip* **2013**, *13*, 2397.

(9) Xu, L. Q.; Neoh, K. G.; Kang, E. T.; Fu, G. D. Rhodamine Derivative-Modified Filter Papers for Colorimetric and Fluorescent Detection of Hg2+ in Aqueous Media. *J. Mater. Chem. A* **2013**, *1*, 2526.

(10) Manori Jayawardanea, B.; Cooa, L.; Cattralla, R. W.; Kolev, S. D. The Use of a Polymer Inclusion Membrane in a Paper-Based Sensor for the Selective Determination of Cu (II). *Anal. Chim. Acta* **2013**, *803*, 106−112.
(11) Hajizadeh, S.; Farhadi, K.; Forough, M.; Sabzi, R. E. Silver Nanoparticles as a Cyanide Colorimetric Sensor in Aqueous Media. *Anal. Methods* **2011**, *3*, 2599−2603.
(12) Tseng, P. J.; Wang, C. Y.; Huang, T. Y.; Chuang, Y. Y.; Fu, S. F.; Lin, Y. W. A Facile Colorimetric Assay for Determination of Salicylic Acid in Tobacco Leaves Using Titanium Dioxide Nanoparticles. *Anal. Methods* **2014**, *6*, 1759−1765.
(13) Cate, D. M.; Dungchai, W.; Cunningham, J. C.; Volckens, J.; Henry, C. S. Simple, Distance-Based Measurement for Paper Analytical Devices. *Lab Chip* **2013**, *13*, 2397−2404.
(14) Xu, M.; Bunes, B. R.; Zang, L. Paper-Based Vapor Detection of Hydrogen Peroxide: Colorimetric Sensing with Tunable Interface. *ACS Appl. Mater. Interfaces* **2011**, *3*, 642−647.
(15) Zargar, B.; Hatamie, A. Colorimetric Determination of Resorcinol Based on Localized Surface Plasmon Resonance of Silver Nanoparticles. *Analyst* **2012**, *137*, 5334−5338.
(16) Hua, C.; Zhang, W. H.; Almeida, S. R.; Ciampi, S.; Gloria, D.; Liu, G.; Harper, J. B.; Gooding, J. J. A Novel Route to Copper (II) Detection Using 'Click' Chemistry-Induced Aggregation of Gold Nanoparticles. *Analyst* **2012**, *137*, 82−86.
(17) Zietz, B. P.; Dieter, H. H.; Lakomek, M.; Schneider, H.; Keßler-Gaedtke, B.; Dunkelberg, H. Epidemiological Investigations on Chronic Copper Toxicity to Children Exposed via the Public Drinking Water Supply. *Sci. Total Environ.* **2003**, *302*, 127−144.
(18) Barnham, K. J.; Masters, C. L.; Bush, A. I. Neurodegenerative Diseases and Oxidative Stress. *Nat. Rev. Drug Discovery* **2004**, *3*, 205−214.
(19) Liu, X.; Zong, C.; Lu, L. Fluorescent Silver Nanoclusters for User-Friendly Detection of Cu^{2+} on a Paper Platform. *Analyst* **2012**, *137*, 2406.
(20) Rice, K. P.; Walker, E. J., Jr.; Stoykovich, M. P.; Saunders, A. E. Solvent-Dependent Surface Plasmon Response and Oxidation of Copper Nanocrystals. *J. Phys. Chem. C* **2011**, *115*, 1793−1799.
(21) Ratnarathorn, N.; Chailapakul, O.; Henry, C. S.; Dungcha, W. Simple Silver Nanoparticle Colorimetric Sensing for Copper by Paper-Based Devices. *Talanta* **2012**, *99*, 552−557.
(22) Lin, Q.; Chen, P.; Liu, J.; Fu, Y. P.; Zhang, Y. M.; Wei, T. B. Colorimetric Chemosensor and Test Kit for Detection Copper(II) Cations in Aqueous Solution with Specific Selectivity and High Sensitivity. *Dyes Pigm.* **2013**, *98*, 100−105.
(23) Kazeminezhad, I.; Sadollahkhani, A. Photocatalytic Degradation of Eriochrome black-T Dye Using ZnO Nanoparticles. *Mater. Lett.* **2014**, *120*, 267−270.
(24) Kanmani, S. S.; Ramachandran, K. Synthesis and Characterization of TiO2/ZnO Core/Shell Nanomaterials for Solar Cell Applications. *Renewable Energy* **2012**, *43*, 149−156.
(25) Fan, J. D.; Fábrega, C.; Zamani, R.; Shavel, A.; Güell, F.; Carrete, A.; Andreu, T.; López, A. M.; Morante, J. R.; Arbiol, J.; Cabot, A. Solution-Qrowth and Optoelectronic Properties of ZnO:Cl@ZnS Core−Shell Nanowires with Tunable Shell Thickness. *J. Alloys Compd.* **2013**, *555*, 213.
(26) Ahn, B. H.; Lee, J. Y. Effects of a Low-Temperature Sulfidation Process on the Microstructural Properties of ZnO Nanowires: ZnS Formation and Nanoscale Kirkendall Effect. *CrystEngComm* **2013**, *15*, 6709−6714.
(27) Nam, W. H.; Lim, Y. S.; Seo, W. S.; Cho, H. K.; Lee, J. Y. Control of the Shell Structure of ZnO−ZnS Core-Shell Structure. *J. Nanopart. Res.* **2011**, *13*, 5825−5831.
(28) Sharma, S.; Chawla, S. Enhanced UV Emission in ZnO/ZnS Core Shell Nanoparticles Prepared by Epitaxial Growth in Solution. *Electron. Mater. Lett.* **2013**, *9*, 267−271.
(29) Liu, S.; Wang, X.; Zhao, W.; Wang, K.; Sang, H. X.; He, Z. Synthesis, Characterization and Enhanced Photocatalytic Performance of Ag_2S-Coupled ZnO/ZnS Core/Shell Nanorods. *J. Alloys Compd.* **2013**, *568*, 84−91.
(30) Wenjiang, L.; Ge, S.; Fei, X.; Minfang, C.; Yue, Z. Preparation of Spherical ZnO/ZnS Core/Shell Particles and the Photocatalytic Activity for Methyl Orange. *Mater. Lett.* **2013**, *96*, 221−223.
(31) Yuan, X.; Chen, Y. Visual Determination of Cu_{2+} through Copper-Catalysed in situ Formation of Ag Nanoparticles. *Analyst* **2012**, *137*, 4516−4523.
(32) Kuo, C. T.; Liu, Y. M.; Wu, S. H.; Lin, C. H.; Lin, C. M.; Chen, C. H. Visual Semiquantification via the Formation of Phase Segregation. *Anal. Chem.* **2011**, *83*, 3765−3769.
(33) Lutfullah; Sharm, S.; Rahman, N.; Hejaz Azmi, S. N.; Iqbal, B.; Bait Amburk, M. I. B.; Al Barwanib, Z. M. UV Spectrophotometric Determination of Cu(II) in Synthetic Mixture and Water Samples. *J. Chin. Chem. Soc.* **2010**, *57*, 622−631.
(34) Zhou, Y.; Wang, S.; Zhang, K.; Jiang, X. Visual Detection of Copper (II) by Azide- and Alkyne-Functionalized Gold Nanoparticles Using Click Chemistry. *Angew. Chem., Int. Ed.* **2008**, *47*, 7454−7456.
(35) Chandrasekhar, V.; Das, S.; Yadav, R.; Hossain, S.; Parihar, R.; Subramaniam, G.; Sen, P. Novel Chemosensor for the Visual Detection of Copper(II) in Aqueous Solution at the ppm Level. *Inorg. Chem.* **2012**, *51* (16), 8664−8666.
(36) Wang, Z.; Wang, M.; Wu, G.; Wu, D.; Wu, A. . Colorimetric Detection of Copper and Efficient Removal of Heavy Metal Ions from Water by Diamine-Functionalized SBA-15. *Dalton Trans.* **2014**, *43*, 8461−8468.
(37) Rodrigues, A.; Brito, A.; Janknecht, P.; Fernanda Proença, M. F.; Nogueira, R. Quantification of Humic Acids in Surface Water: Effects of Divalent Cations, pH, and Filtration. *J. Environ. Monit.* **2009**, *11*, 377−382.
(38) Kostic, I.; Andelkovic, T.; Nikolic, R.; Bojic, A.; Purenovic, M.; Blagojevic, S.; Andelkovic, D. Copper(II) and lead(II) Complexation by Humic Acid and Humic-Like Ligands. *J. Serb. Chem. Soc.* **2011**, *76* (9), 1325−1336.
(39) Senapati, U. S.; Jha, D. K.; Sarkar, D. Green Synthesis and Characterization of ZnS Nanoparticles. *Res. J. Physical Sci.* **2013**, *1*, 1−6.
(40) Shuai, X. M.; Shen, W. Z. A Facile Chemical Conversion Synthesis of ZnO/ZnS Core/Shell Nanorods and Diverse Metal Sulfide Nanotubes. *J. Phys. Chem. C* **2011**, *115*, 6415−6422.
(41) Zhu, Y. F.; Fan, D. H.; Shen, W. Z. A General Chemical Conversion Route to Synthesize Various ZnO-Based Core/Shell Structures. *J. Phys. Chem. C* **2008**, *112*, 10402−10406.
(42) Lubeck, C. R.; Han, T. Y.; Gash, A. E.; Satcher, J. H., Jr.; Doyle, F. M. Synthesis of Mesostructured Copper Sulfide by Cation Exchange and Liquid-Crystal Templating. *Adv. Mater.* **2006**, *18*, 781−784.